Dalton Transactions

PAPER

View Article Online
View Journal | View Issue

Cite this: *Dalton Trans.*, 2019, **48**, 9276

Phosphorescence enhancement by close metal–metal interaction in T_1 excited state in a dinuclear copper(I) complex†

Simona Bassoli,[a] G. Attilio Ardizzoia,[a] Bruno Therrien[b] and Stefano Brenna*[a]

Received 12th April 2019,
Accepted 29th May 2019

DOI: 10.1039/c9dt01565e

rsc.li/dalton

The dinuclear copper(I) complex $[Cu_2(\mu\text{-dppm})_2(lact)(\mu\text{-lact})]$ (**1**) (dppm = bis(diphenylphosphino) methane; lact = L-(+)-lactate) was synthesized and fully characterized both in solution and solid state. Variable temperature NMR experiments (^1H and ^{31}P), conductivity measurements and infrared spectroscopy, suggest the occurrence of a fluxional behavior in solution involving the lactate anion. The crystal structure shows the presence of both monodentate and bridged lactate in the complex. In the solid state, **1** shows green phosphorescent emission characterized by a very large Stokes shift (161 nm, 1.09 eV) and a good absolute quantum yield (0.43). Calculations performed at the Density Functional Theory level demonstrate that the electronic transition responsible for the emission originates from a triplet excited state where the shortening of the Cu···Cu distance plays a crucial role.

Introduction

Luminescent complexes based on metals with d^{10} configuration have received significant attention in the last decades, as they are good alternatives to those based on the more expensive platinum group metals (PGMs).[1,2] Indeed, relevant reports have already appeared in the literature regarding the use of Zn(II)[3] and Cu(I)[4–6] systems in the fabrication of OLEDs or DSSCs. In particular, copper(I) complexes are widely investigated because of their structural versatility which leads to efficient luminescent materials.[7,8] For example, one peculiar photophysical property of copper(I) derivatives is the thermally activated delayed fluorescence (TADF), which originates from a small energy difference between the singlet and triplet excited states.[9,10] The most investigated systems are $[Cu(phen)_2]^+$ (phen = substituted 1,10-phenantroline) or mixed $[Cu(NN)(PP)]^+$ species, where NN and PP indicate respectively, a 2,9-disubstituted 1,10-phenantroline and a diphosphine. Usually, the introduction of bulky groups close to the nitrogen heterocycle[8] and the use of a rigid PP ligand (like bis[(2-diphenylphosphino)phenyl] ether)[10] reduces the structural distortions of the excited state, consequently increasing luminescence quantum yield and the overall efficiency. In addition, mixed trigonal CuP_2N or tetrahedral CuP_2N_2 complexes with monodentate phosphines led to remarkable results, as documented by recent papers from Kato and coworkers.[11,12]

In our ongoing exploration on complexes with nitrogen-containing ligands,[13–16] we investigated the behavior of luminescent d^{10}-metal compounds, first focusing our attention on zinc(II)[17–19] and silver(I)[20] complexes bearing bidentate imidazo-pyridine ligands. Then, we also studied the phosphorescent behavior of a copper(I) coordination polymer with sodium 3,5-dimethyl-4-sulfonate pyrazolate as ligand.[21] More recently, we synthesized the mixed ligand copper(I) species $[Cu(PPh_3)_2(lact)]$ (lact = L-(+)-lactate)[22] which showed phosphorescence in the solid state. X-ray diffraction analysis revealed how the α-hydroxycarboxylate ligand was involved in intermolecular hydrogen bonds whose arrangement strongly affected the emissive properties of the complex. Unfortunately, $[Cu(PPh_3)_2(lact)]$ suffered from a low quantum yield (0.14). Thus, we proceeded with the substitution of PPh_3 with bis(diphenylphosphino)methane (dppm), which is known to act as bridging bidentate phosphane ligand generating quite rigid $\{Cu_2(\mu\text{-dppm})_2\}^{2+}$ systems.[23–25] This rigidity usually enhances luminescence when compared to compounds with monodentate phosphines.[26,27]

Herein, we present the reaction of the above mentioned complex $[Cu(PPh_3)_2(lact)]$ with dppm, to generate the dinuclear system $[Cu_2(\mu\text{-dppm})_2(lact)(\mu\text{-lact})]$ (**1**), in which the lactate anions show two different coordination modes. The construc-

[a]*Dipartimento di Scienza e Alta Tecnologia, Università degli Studi dell'Insubria and CIRCC, Via Valleggio, 9 - 22100 Como, Italy. E-mail: stefano.brenna@uninsubria.it; Fax: +39-(0)31-2386119; Tel: +39-(0)31-2386476*

[b]*Institute of Chemistry, Université de Neuchâtel, Avenue de Bellevaux 51, CH-2000 Neuchâtel, Switzerland*

†Electronic supplementary information (ESI) available: Infrared, ^1H, ^{13}C and ^{31}P NMR spectra of complex **1**; fitting of the lifetime decay curve of complex **1**; frontier molecular orbitals for S_0, S_1 and T_1 states; optimized S_0, S_1 and T_1 geometries for compound **1**; crystallographic and structure refinement parameters for compound **1**; spectroscopic data for compound **1** recorded in acetone (77 K). CCDC 1907943. For ESI and crystallographic data in CIF or other electronic format see DOI: 10.1039/c9dt01565e

tion of an eight membered $Cu_2(PCP)_2$ cycle increases structural rigidity, resulting in remarkable phosphorescence characterized by a high Stokes shift and a good absolute quantum yield. According to TD-DFT calculations, the strong phosphorescence is the result of a $^3(Cu_2)$LCT electronic transition in the triplet (T_1) excited state generated by a close interaction between the two copper(I) atoms. The dinuclear disposition in compound **1** is maintained in solution, as established by NMR and IR experiments. However, a fluxional mechanism involving the lactate anions prevents any luminescence in solution.

Results and discussion

Synthesis and solid state characterization

Compound $[Cu_2(\mu\text{-dppm})_2(lact)(\mu\text{-lact})]$ (dppm = bis(diphenylphosphino)methane; lact = L-(+)-lactate) (**1**) was synthesized by suspending $[Cu(PPh_3)_2(lact)]$ in diethyl ether, in the presence of one equivalent of dppm (Scheme 1). The formulation of the complex with a 1 : 1 : 1 Cu : dppm : lactate ratio was first designated according to elemental analysis.

The infrared spectrum of **1** (Fig. 1) is characterized by a sharp band at 1096 cm^{-1} due to bound dppm, three stretching frequencies at 1609, 1577 and 1568 cm^{-1} (ν_{asymm} COO) and one at 1434 cm^{-1} (ν_{symm} COO) assigned to the lactate. The two broad bands at 3393 and 3312 cm^{-1} (Fig. S1†) are attributed to OH groups of lactate, reasonably not involved in H-bonds. The three intense and different stretching frequencies associated to carboxylate groups are indicative of the presence of two dissimilar bound lactate: the upper (1609 cm^{-1}) and the lower (1568 cm^{-1}) are representative of a monodentate carboxylate, whereas the central frequency indicates a bridging disposition *via* the two oxygen atoms of the carboxylate group (Fig. 1).

X-ray structural investigation

X-ray quality crystals of complex $[Cu_2(\mu\text{-dppm})_2(lact)(\mu\text{-lact})]$ (**1**) were obtained by layering diethyl ether on a saturated dichloromethane solution of **1**. The compound crystallizes in the triclinic space group *P*1 with two independent molecules per unit cell (labeled A and B). As predicted by infrared spectroscopy, the structure of **1** shows two differently bound lactate anions, one coordinated to copper in a monodentate mode

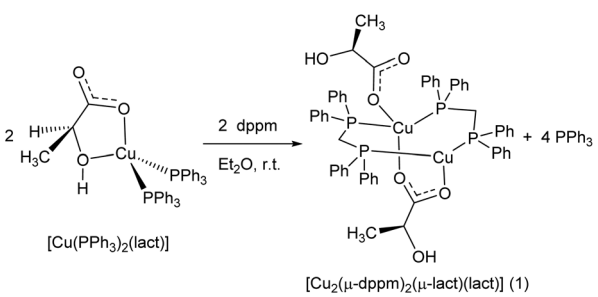

Scheme 1 Synthesis of the dinuclear complex $[Cu_2(\mu\text{-dppm})_2(lact)(\mu\text{-lact})]$ (dppm = bis(diphenylphosphino)methane; lact = L-(+)-lactate) (**1**).

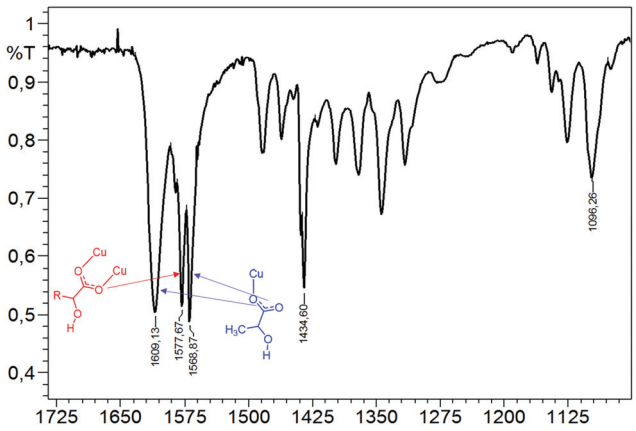

Fig. 1 Infrared spectrum (ATR) of compound **1** with the three different asymmetric stretching frequencies of lactate (ν_{asymm} COO) being highlighted.

and the second bridging two copper atoms (Fig. 2). The structure and the geometrical parameters of the two symmetrically independent complexes are quite similar, as emphasized in Fig. 2. Indeed, despite a different orientation of the phenyl groups of the dppm ligands, the distances and angles surrounding the Cu(I) atoms are almost identical (see Table 1), thus having most likely the same electronic properties.

Interestingly, in the dinuclear complex, the copper atoms possess different coordination geometries, trigonal and tetrahedral respectively. The copper with a distorted trigonal geometry shows an average P–Cu–P angle of 140.7° and O–Cu–P angles of 108.5°. The atoms defining the CuP_2O plane are coplanar, with the root mean square deviation of the fitted atoms being 0.072 (Mol A) and 0.084 (Mol B) respectively. On the other hand, the copper atom in a tetrahedral environment has an average P–Cu–P angle of 122.8°, a O–Cu–O angle of 92.7° and O–Cu–P angles comprise between 98.9° and 117.8°. The calculated geometry index[28] for the tetrahedral centers are respectively 0.92 (Mol A) and 0.68 (Mol B). Such dinuclear systems with mixed trigonal and tetrahedral copper centers are relatively common in the literature.[23,29–38]

The overall arrangement of complex **1** is composed of two fused octa-atomic cycles, respectively described as Cu–P–C–P–Cu–P–C–P and Cu–P–C–P–Cu–O–C–O (Fig. S2†). The $\{Cu_2(\mu\text{-dppm})_2\}^{2+}$ unit shows a distorted boat–chair conformation, with Cu···Cu distances of 2.892(1) Å and 2.846(1) Å, respectively. These distances are just above the sum of the van der Waals radii for two copper(I) atoms (2.80 Å).[39] Consequently, these values appear to be among the shortest observed for $\{Cu_2(\mu\text{-dppm})_2\}^{2+}$ units.[40] Finally, no meaningful intermolecular interactions are observed in the crystal, despite the presence of the hydroxyl group of the mono-coordinated lactate anion at the periphery of complex **1**. Nevertheless, a weak intramolecular interaction between the carboxylate of the monodentate lactate and the hydroxyl group of the bridging lactate is observed.

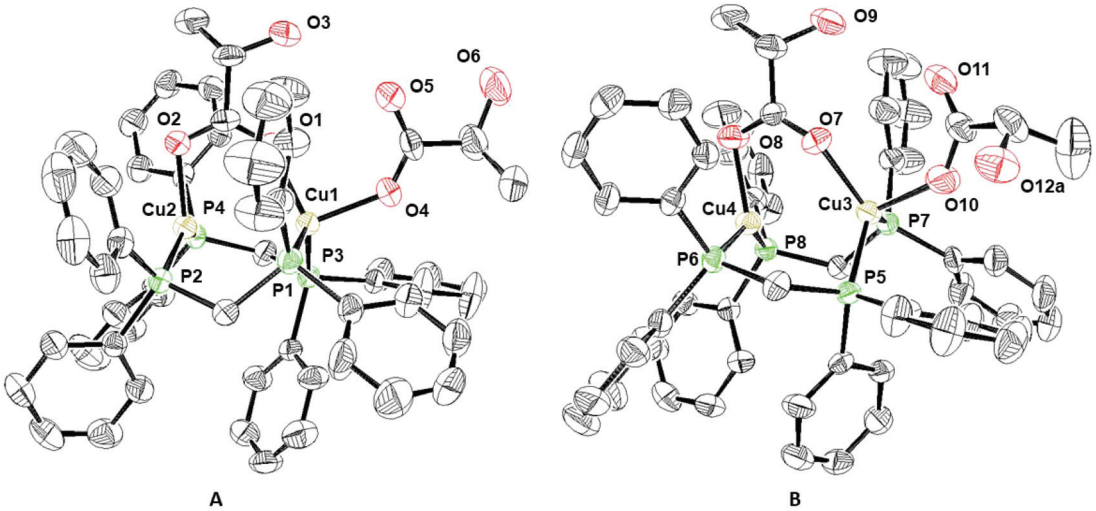

Fig. 2 Molecular structure of $[Cu_2(\mu\text{-dppm})_2(lact)(\mu\text{-lact})]$ (**1**) at 50% probability level ellipsoids, both symmetrically independent complexes are presented (Mol A and Mol B). Only one orientation of the disordered terminal lactate anion in Mol B is presented.

Table 1 Selected bond distances (Å) and angles (°) in the X-ray crystal structure of **1** (Mol A, Mol B, average) and in the optimized geometries for S_0, S_1 and T_1; Mol A and Mol B refer to the two independent complexes of **1** per unit cell

	Mol A	Mol B	avg	S_0 opt	S_1 opt	T_1 opt
Cu–Cu	2.892(1)	2.846(1)	2.87	2.93	3.16	2.71
Cu1–P1	2.237(2)	2.255(2)	2.25	2.27	2.36	2.31
Cu1–P3	2.240(2)	2.228(2)	2.23	2.26	2.27	2.25
Cu2–P2	2.206(2)	2.224(2)	2.21	2.25	2.30	2.33
Cu2–P4	2.223(2)	2.191(2)	2.21	2.23	2.24	2.22
P1–P2	3.017(3)	3.021(3)	3.02	3.10	3.16	3.11
P3–P4	3.038(3)	3.007(3)	3.02	3.05	3.13	3.04
P1–Cu–P3	123.34(9)	122.24(9)	122.8	116.7	105.6	104.9
P2–Cu–P4	140.21(9)	141.22(9)	140.7	134.7	136.3	131.3

Solution study

First, an NMR inspection (^1H, ^{13}C and $^{31}P\{^1H\}$) was performed to establish whether the dinuclear triply-bridged structure of complex **1** was maintained in solution. The ^1H NMR spectrum recorded in acetone-d_6 at 20 °C (Fig. S3†) shows the signals of lactate centered at 1.30 (CH_3) and 3.99 ppm (CH), respectively appearing as a doublet ($^3J_{H,H}$ = 6.8 Hz, CH_3) and a broad, not well resolved quartet ($^3J_{H,H}$ = 6.9 Hz, CH). The methylene protons of dppm are found as a broad singlet at 3.54 ppm. The corresponding signals in the ^{13}C NMR spectrum (Fig. S4†) are found at 69.36 (CH), 22.86 (CH_3) and 27.73 ppm (CH_2). In the ^{31}P NMR spectrum (Fig. S7†), one singlet centered at −13.52 ppm is detected, as expected for a distorted boat–chair conformation.[40] These simplified patterns in ^1H and ^{31}P NMR spectra are in contrast with what expected for the dinuclear, asymmetric species described above: the two distinct surroundings around the copper atoms should generate multiple signals for the lactate anions and especially for phosphorous atoms, hence a more complicated pattern would be more plausible in both ^1H and ^{31}P NMR spectra. It is clear that what observed in solution is a different and more symmetric situation compared to the one detected in the solid state, as already reported for other copper(I)-dppm systems with carboxylate ligands.[41] Various possibilities have been considered to elucidate this point. A fast fluxional mechanism involving the lactate ions (blue arrows in Scheme 2) could be operating, where the original bridging lactate molecule would next result as monodentate, and the reverse situation observed for the initial monodentate lactate which would now bridge over the two copper atoms.

Alternatively, once dissolved in solution compound **1** could experience a complete dissociation of the monodentate lactate (Scheme 2, red arrow) eventually leading to an ionic species (Scheme 2, bottom). Again, the geometry and coordination environment around copper atoms in this salt would be identical, in accordance to NMR evidences. In order to clarify the real situation occurring, we first performed conductivity measurements on a diluted (10^{-4} M) acetone solution of compound **1**. Interestingly, no conductivity was detected, the molar conductivity, Λ_M, being 26.1 ohm^{-1} cm^2 mol^{-1}, well below the range expected for a 1 : 1 type electrolyte in the same solvent (100–140 ohm^{-1} cm^2 mol^{-1}).[42] Thus, the formation of a salt could be excluded. Infrared spectroscopy corroborated the existence of a dinuclear compound also in solution, maybe involved in a fast equilibrium: the IR spectrum of $[Cu_2(\mu\text{-dppm})_2(lact)(\mu\text{-lact})]$ dissolved in CH_2Cl_2 shows a similar

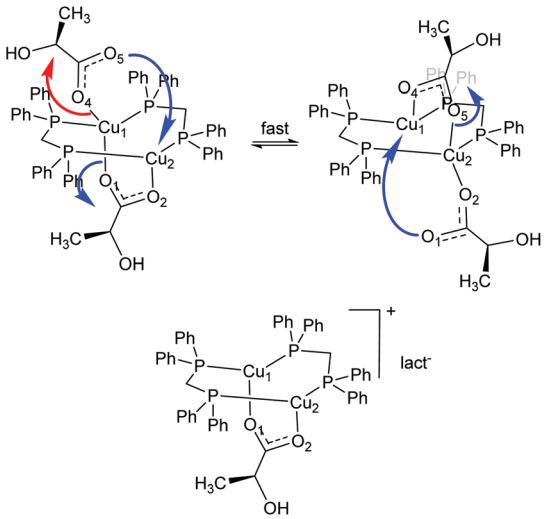

Scheme 2 Possible symmetrical arrangements around the copper atoms in solution.

pattern as in solid state, with three intense frequencies at 1608, 1585 and 1571 cm^{-1} (Fig. S8†). Then, compound **1** retains its dinuclear arrangement even in solution, with the two lactate anions continuously exchanging their coordination mode from monodentate to bridged at room temperature.

This condition persists even at low temperatures (213 K), as demonstrated by VT ^{1}H and $^{31}P\{^{1}H\}$ NMR experiments (Fig. S9 and S10†). Indeed, it is clearly visible from ^{1}H NMR spectra (Fig. S9†) how the singlet of methylene protons slightly shifts to low field and progressively broaden on lowering the temperature. At 213 K, the coalescence is reached, and the signal appears very broad, centered at about 3.75 ppm. Unfortunately, it was not possible to further reduce the temperature in the course of our experiments. The signals from the lactate do not change in the range 298–213 K, only the quartet associated to CH becomes better resolved between 283 and 263 K. The VT $^{31}P\{^{1}H\}$ does not exhibit any significant variation in all the range examined (Fig. S10†). This means that the fluxional mechanism involving the lactate anions as described above, despite slowed down, is reasonably still present in the range investigated, in accordance with phosphorescence measurements (*vide infra*).

Phosphorescent behavior in the solid state

When irradiated with UV light the dinuclear compound $[Cu_2(\mu\text{-dppm})_2(lact)(\mu\text{-lact})]$ (**1**) shows a broad, unstructured emission in the green region, with λ_{max} centered at 516 nm (λ_{exc} = 355 nm). A large Stokes shift of 1.09 eV (8789.2 cm^{-1}) is observed (Table 2, Fig. 3), with a very small superposition between excitation and emission traces. The time-resolved luminescence behavior of complex **1** can be described by a mono-exponential decay with τ = 29.5 μs (Fig. S11†), denoting a phosphorescent emission from a triplet excited state. A significant absolute quantum yield was also measured (Φ_{PL} = 0.43), which is three times higher than the value recorded for the precursor $[Cu(PPh_3)_2(lact)]$ (Φ_{PL} = 0.14).[22] This suggests that the substitution of PPh_3 molecules with bridging dppm ligands provides rigidity to the system and strengthen cuprophilic interactions (absent in the precursor), which eventually enhance phosphorescence.

The phosphorescence of the dinuclear $[Cu_2(\mu\text{-dppm})_2(lact)(\mu\text{-lact})]$ is not maintained in solution, as demonstrated by measurements performed on dichloromethane or acetone solutions of **1**. This lack of emission in solution can reasonably be attributed to the aforesaid fluxional behavior involving the lactate anions, which concomitantly weakens the cuprophilic interaction between the copper atoms, and increases the possibility to experience non-radiative thermal paths, with a resulting absence of emission.

As a proof, starting from an acetone solution of **1**, when the solvent is removed so that solid $[Cu_2(\mu\text{-dppm})_2(lact)(\mu\text{-lact})]$ is recovered, the original phosphorescence is restored. As well, low temperature measurements corroborated this hypothesis: indeed, the lack of emission is still observed when a solution of **1** in acetone or dichloromethane is cooled to 203 K, in accordance with NMR results showing the persistence of fluxionality close to that temperature (213 K). On the contrary, the phosphorescence becomes appreciable when spectra were recorded as a frozen glass at 77 K (Fig. S12†), where certainly the interexchange mechanism involving lactate anions is

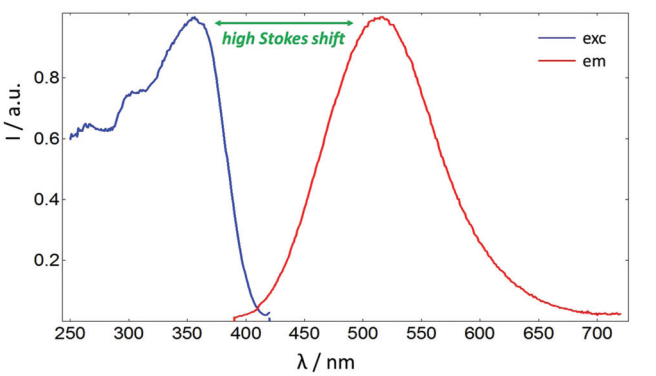

Fig. 3 Normalized excitation and emission spectra of compound $[Cu_2(\mu\text{-dppm})_2(lact)(\mu\text{-lact})]$ (**1**) in the solid state.

Table 2 Photophysical data for compound **1** recorded in the solid state

			Stokes shift						
λ_{abs} (nm)	λ_{exc} (nm)	λ_{em} (nm)	(nm)	(cm^{-1})	(eV)	Φ_{PL}	τ (μs)	k_r ($\times 10^4$ s^{-1})	k_{nr} ($\times 10^4$ s^{-1})
328	355	516	161	8789.2	1.09	0.43	29.5	1.46	1.93

blocked. The emission spectrum of compound **1** in acetone at 77 K is characterized by a structureless band (Fig. S12†) with λ_{max} = 441 nm (λ_{exc} = 337 nm, Table S1†). The hypsochromic shift of the emission of a glassy solution with respect to the room temperature solid state emission (516 nm, Table 2) is not unusual for copper(I) complexes,[7,9,43–45] and the one-order magnitude increase in lifetime after cooling to 77 K (τ_{av} = 171.8 μs *vs*. 29.5 μs, Table S1†) is expected as well.[7,9,43]

DFT calculations

A truthful inspection by TD-DFT calculations allowed to define the nature of the main electronic transitions responsible for absorption and phosphorescence. First, a geometry optimization performed starting from the X-ray data allowed to describe the singlet ground state (S_0): the optimized structure shows bond lengths close to the X-ray values (Table 1) and P–Cu–P angles which are slightly smaller compared to crystal structure. In particular, the Cu···Cu interaction results 2.90 Å, nearly identical to the one observed in the solid state (2.88 Å). Also the calculated UV spectrum of compound **1** in the solid state shows a good correspondence with the experimental trace (Fig. S13†), and allows to identify the $S_0 \rightarrow S_1$ absorption as a HOMO–LUMO (>98%) electronic transfer. The HOMO (Fig. S13†) is mainly localized on one copper atom and one phosphorous atom of two adjacent dppm ligands, whereas the LUMO shows a prevalent contribution from the diphosphine ligand, thus the $S_0 \rightarrow S_1$ transition has a mixed metal–ligand to ligand charge transfer (^{1}MMLLCT) character.[46–48] In the optimized singlet excited state (S_1), the bond distances are longer than in the ground state (Table 1) and especially the interaction between copper atoms is considerably lengthened to 3.16 Å. The P–Cu–P angles become smaller than in S_0. The frontier molecular orbitals show similar shape compared to S_0, once again with an admixed metal–ligand character for the HOMO and a LUMO entirely localized on the P–Ph bond of the diphosphine (Fig. S14†).

Since the phosphorescence of compound **1** derives from a triplet excited state, reasonably after the $S_0 \rightarrow S_1$ absorption an intersystem crossing (ISC) process to a triplet excited state occurs, eventually leading to the emission. Thus, we performed geometry optimization for the T_1 state as well, particularly to assess any possible influence of a cuprophilic interaction in the luminescent behavior. Interestingly, the Cu···Cu distance in T_1 is significantly shortened to 2.71 Å (to be compared with 2.88 Å (X-ray) and 3.16 (optimized S_1)). Moreover, the P–Cu–P angles are the narrowest in the series: P1–Cu–P3 and P2–Cu–P4 respectively measuring 104.9° and 131.3°, while being 122.8° and 140.7° in the crystal structure and 105.6° and 136.3° in S_1 (Table 1).

Such a shortening of metallophilic contacts in the excited state are common for dinuclear[49–54] and polynuclear[55] coinage metal compounds. In particular, in the case of phosphorescent dinuclear species the electronic transition responsible for emission from the triplet state is either described as $^3[n\mathrm{d}\sigma^* \rightarrow (n+1)\mathrm{p}\sigma]$[50,56] or as ^{3}(M,M′)LCT[52,54] according to DFT results. Usually, when only silver(I) or gold(I) metal centers are involved, $^3[4\mathrm{d}\sigma^* \rightarrow 5\mathrm{p}\sigma]$ or $^3[5\mathrm{d}\sigma^* \rightarrow 6\mathrm{p}\sigma]$ character is observed for the triplet state transition.[50] Otherwise, in the presence of copper(I) centers, the electronic transition in the triplet state (T_1) usually shows a high contribution from the metallophilic contacts, which are rather shorter than in the ground state. Indeed, the HOMO in the T_1 state is mainly located within the two copper centers, whereas the LUMO lies on the bound ligand, so that the transition is defined as $^3(M_2)$LCT (M = Cu).[52] Our case is similar to those reported in the literature for such copper(I) dinuclear complexes: as said, in the T_1 state a noticeable shortening of the Cu···Cu distance is observed;

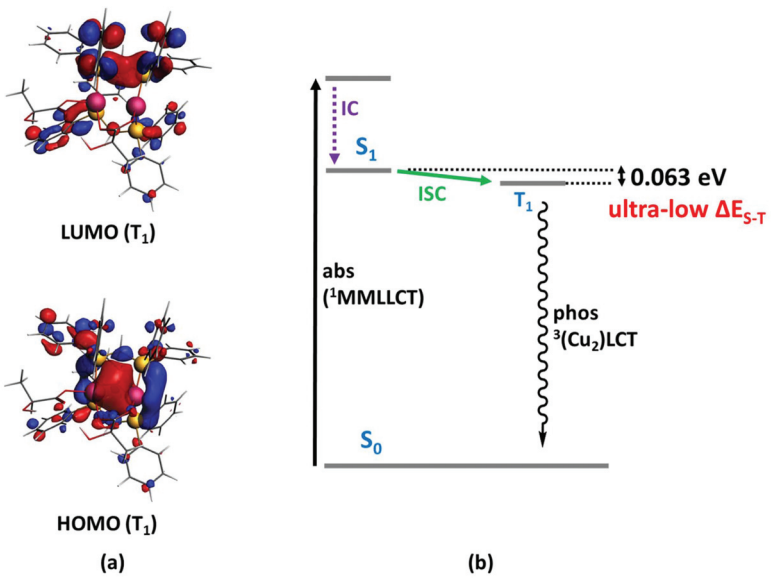

Fig. 4 (a) Highest occupied molecular orbital (HOMO (T_1)) and lowest unoccupied molecular orbital (LUMO (T_1)) calculated for the triplet excited state (T_1) of compound **1**; (b) schematic representation of the process involving $S_0 \rightarrow S_1$ and $T_1 \rightarrow S_0$ transitions.

moreover, when looking at the frontier molecular orbitals calculated for the triplet state (HOMO(T_1) and LUMO(T_1), Fig. 4a), the electron density between the two metal atoms indicative of a close Cu···Cu contact is clearly visible in HOMO (T_1). In the LUMO(T_1) the density moves to one bridging dppm ligand (Fig. 4a) thus, following the aforementioned notation, the transition responsible for the phosphorescence in compound **1** can be described as ^{3}(Cu_2)LCT. As known, increasing the Cu···Cu bond order in the excited state enhances the spin–orbit coupling (SOC), which then favors intersystem crossing (ISC) from S_1 to T_1 state, in our case also boosted by the ultra-low energy gap between the singlet and the triplet excited states (ΔE_{S-T} = 0.063 eV, Fig. 4b). Spectroscopic and calculated data (*i.e.*, τ and ΔE_{S-T}) are also in accordance with those reported for similar dinuclear copper(I) complexes having the same ^{3}(Cu_2)LCT phosphorescence path.[52,54] To sum up, a vertical $S_0 \rightarrow S_1$ absorption with ^{1}MMLLCT character, followed by internal conversion (IC), populates the vibrational ground state of S_1. Then, an intersystem crossing (ISC) to the excited triplet state T_1 occurs, which is favored by the strong spin orbit coupling (SOC) experienced by the copper(I) atoms due to a marked cuprophilic interaction in the T_1 state. In relaxing to S_0, electron density moves from the metal–metal contact (Cu_2) to one adjacent bridging dppm ligand (L), so that the charge transfer transition is defined as ^{3}(Cu_2)LCT.

Conclusions

The synthesis of a mixed ligand phosphorescent copper(I) compound with lactate and bis(diphenylphosphino)methane (dppm) was presented. The X-ray crystal structure analysis showed the bridging disposition of dppm and the presence of two differently bound α-hydroxycarboxylate ligands (monodentate and bridging). This results in the formation of a dinuclear, asymmetric copper complex. Solution studies clearly demonstrated that this dinuclear arrangement is maintained in solution, where the two lactate anions undergo a fast fluxional exchange mechanism at room temperature. In the solid state, the title compound shows intense phosphorescent, green emission, which disappears once the compound is dissolved in organic solvents as a consequence of the fluxionality concerning lactate. TD-DFT calculations demonstrated that phosphorescence originates from the shortening of the copper–copper contacts in the excited triplet state. Thus, the substitution of the two molecules of PPh_3 in the precursor [Cu(PPh_3)$_2$(lact)] with the bridging dppm ligand, increased the rigidity in the dinuclear title compound, with a consequent enhancement of the emissive properties.

Materials and methods

General remarks

All reactions were carried out under nitrogen using standard Schlenk techniques. Solvents were dried and distilled according to standard procedures prior to use. NMR spectra were recorded with an AVANCE 400 Bruker spectrometer at 400 MHz for ^{1}H NMR, 100 MHz for ^{13}C and 162 MHz for ^{31}P{^{1}H} NMR. Chemical shifts are given as δ values in ppm relative to residual solvent peaks as the internal reference (for ^{1}H and ^{13}C NMR) and to external H_3PO_4 (85%) (for ^{31}P NMR). *J* values are given in Hz. Elemental analyses were obtained with a PerkinElmer CHN Analyzer 2400 Series II. Infrared Spectra were acquired on a Shimadzu Prestige-21 spectrophotometer with a 1 cm^{-1} resolution. The excitation and emission spectra were acquired with an Edinburgh Instrument FS5 spectrophotometer equipped with a 150 W continuous Xenon lamp as a light source and were corrected for the wavelength response of the instrument; lifetime measurements were performed on the same FS5 Edinburgh Instrument equipped with a LLS-310 Ocean Optics LED Light Source (wavelength 310 nm; FWHM 12 nm; power 15 μW) as the pulsed source. Analysis of the lifetime decay curve was performed using Fluoracle® Software package (Ver. 1.9.1) which runs the FS5 Edinburgh Instrument. Absolute fluorescence quantum yields were determined on a Photon Technologies International QuantaMaster QM-40 spectrophotometer (equipped with Xe arc lamp, 70 W) using a PhotoMed GmbH K-Sphere Integrating Sphere (3.2 inch. diameter). [Cu(PPh_3)$_2$(lact)] was prepared as previously reported.[22] All other chemicals were of reagent grade quality, were purchased from commercial sources (TCI Chemicals, Acros, AlfaAesar), and used as received.

Synthesis of [Cu_2(μ-dppm)$_2$(lact)(μ-lact)] (1)

A 100 mL Schlenk flask was equipped with a Schlenk glass filter charged with about 2 g of Al_2O_3. Then 40 mL of diethyl ether were added to the filter, and nitrogen gas was inflated from below so that the solvent could be deoxygenated while mixed with alumina. Then the nitrogen flow was stopped and the solvent was left to leach into the flask. In another flask, 0.142 g (0.369 mmol) of bis(diphenylphosphino)methane (dppm) were dissolved in 15 mL of the previously deoxygenated diethyl ether, and 0.250 g (0.369 mmol) of [Cu(PPh_3)$_2$(lact)] were added. The white suspension was vigorously stirred at 20 °C for 24 h. After filtration, the solid was thoroughly washed with deoxygenated diethyl ether and dried *in vacuo*. The copper(I) product is highly stable in the solid state, and was stored under air. Yield: 0.115 g (58%). IR (ATR, ν/cm^{-1}): 3393 (OH), 3312 (OH), 1609 (lact), 1577 (lact), 1565 (lact), 1096 (dppm). IR (CH_2Cl_2 solution, ν/cm^{-1}): 1608 (lact), 1585 (lact), 1571 (lact). Anal. Calc. for $C_{56}H_{54}Cu_2O_6P_4$: C, 62.63; H, 5.07. Found: C, 62.78; H, 5.19. ^{1}H NMR (400 MHz, acetone-d_6, 25 °C): δ = 1.30 (d, $J_{H,H}$ = 6.8 Hz, 3H, CH_3), 3.54 (s, 2H, CH_2P), 3.99 (br q, $J_{H,H}$ = 6.9 Hz, 1H, C*H*), 7.05 (t, $J_{H,H}$ = 7.2 Hz, 1H, Ar–H_m), 7.19 (t, $J_{H,H}$ = 7.4 Hz, 1H, Ar–H_p), 7.56 (t, $J_{H,H}$ = 7.2 Hz, 1H, Ar–H_o). ^{13}C NMR (100 MHz, acetone-d_6, 25 °C): 22.86 (*C*H_3), 27.73 (*C*H_2), 69.36 (*C*H), 129.73 (Ar–CH^{meta}), 131.16 (Ar–*C*H_p), 134.58 (Ar–CH^{ortho}), 135.37 (Ar–C^{ipso}) (it was not possible to identify the NMR signal of the other quaternary carbons). ^{31}P NMR (162 MHz, acetone-d_6, 25 °C): δ = −13.52.

Single-crystal X-ray structure analysis

A crystal of compound **1** was mounted on a Stoe Image Plate Diffraction system equipped with a ϕ circle goniometer, using Mo-Kα graphite monochromated radiation (λ = 0.71073 Å) with ϕ range 0–200°. The structure was solved by direct methods using the program SHELXS, while refinement and all further calculations were carried out using SHELXL.[57] The H-atoms were included in calculated positions and treated as riding atoms using the SHELXL default parameters. The non-H atoms were refined anisotropically, using weighted full-matrix least-square on F^2. In molecule B, the monodentate lactate anion is disordered over two positions with a 0.664 and 0.336 occupancies. Crystallographic details are summarized in Table S2.† Fig. 2 was drawn with ORTEP-32.[58]

CCDC 1907943† contains the supplementary crystallographic data for this paper.

Computational details

All calculations were carried out at the density functional (DFT) level of theory with the ADF2017.113 program package.[59] The PBE functional plus a D3 dispersion correction energy term (PBE-D3)[60] was employed for all calculations. For geometry optimizations, the C, H, O and P atoms were described through TZ2P basis sets [triple-ζ Slater-type orbitals (STOs) plus two polarization function]; the QZ4P basis set (quadruple-ζ STO plus four polarization functions) was used for Cu atoms. The corresponding augmented basis set[61] was employed in TD-DFT calculations: the 40 lowest singlet–singlet and singlet–triplet excitations were calculated by using the optimized geometry. No-frozen-core approximation (all electron) and no-symmetry constrains were used in all calculations.

Conflicts of interest

There are no conflicts to declare.

Acknowledgements

S. B. and G. A. A. thank the Ministero dell'Università e della Ricerca (MIUR) and the University of Insubria for financial support. Fondazione Banca del Monte di Lombardia (FBML) is greatly acknowledged for generous funding through the Research Project "Transition-metals based coordination compounds for light emitting device applications". Prof. A. Maspero is greatly acknowledged for performing VT NMR experiments. Dr Sara Durini is acknowledged for experimental assistance.

Notes and references

1 V. Yam and K. K.-W. Lo, *Chem. Soc. Rev.*, 1999, **28**, 323–334.
2 A. Barbieri, G. Accorsi and N. Armaroli, *Chem. Commun.*, 2008, 2185–2193.
3 G. Cheng, G. K.-M. So, W.-P. To, Y. Chen, C.-C. Kwok, C. Ma, X. Guan, X. Chang, W.-M. Kwoke and C.-M. Che, *Chem. Sci.*, 2015, **6**, 4623–4635.
4 S. Y. Brauchli, B. Bozic-Weber, E. C. Constable, N. Hostettler, C. E. Housecroft and J. A. Zampese, *RSC Adv.*, 2014, **4**, 34801–34815.
5 M. Wallesch, A. Verma, C. Fléchon, H. Flügge, D. M. Zink, S. M. Seifermann, J. M. Navarro, T. Vitova, J. Göttlicher, R. Steininger, L. Weinhardt, M. Zimmer, M. Gerhards, C. Heske, S. Bräse, T. Baumann and D. Volz, *Chem. – Eur. J.*, 2016, **22**, 16400–16405.
6 D. Volz, Y. Chen, M. Wallesch, R. Liu, C. Fléchon, D. M. Zink, J. Friedrichs, H. Flügge, R. Steininger, J. Göttlicher, C. Heske, L. Weinhardt, S. Bräse, F. So and T. Baumann, *Adv. Mater.*, 2015, **27**, 2538–2543.
7 M. J. Leitl, D. M. Zink, A. Schinabeck, T. Baumann, D. Volz and H. Yersin, *Top. Curr. Chem. (Z)*, 2016, **347**, 25.
8 A. Kobayashi and M. Kato, *Chem. Lett.*, 2017, **46**, 154–162.
9 R. Hamze, J. L. Peltier, D. Sylvinson, M. Jung, J. Cardenas, R. Haiges, M. Soleilhavoup, R. Jazzar, P. I. Djurovich, G. Bertrand and M. E. Thompson, *Science*, 2019, **363**, 601–606.
10 R. Czerwieniec, M. J. Leitl, H. H. H. Homeier and H. Yersin, *Coord. Chem. Rev.*, 2016, **325**, 2–28.
11 P. Liang, A. Kobayashi, T. Hasegawa, M. Yoshida and M. Kato, *Eur. J. Inorg. Chem.*, 2017, 5134–5142.
12 A. Kobayashi, R. Arata, T. Ogawa, M. Yoshida and M. Kato, *Inorg. Chem.*, 2017, **56**, 4280–4288.
13 G. A. Ardizzoia, S. Brenna and B. Therrien, *Eur. J. Inorg. Chem.*, 2010, 3365–3371.
14 D. Tzimopoulos, S. Brenna, A. Czapik, M. Gdaniec, A. Ardizzoia and P. D. Akrivos, *Inorg. Chim. Acta*, 2012, **383**, 105–111.
15 G. A. Ardizzoia, S. Brenna, S. Durini, I. Trentin and B. Therrien, *Dalton Trans.*, 2013, **42**, 12265–12273.
16 G. A. Ardizzoia and S. Brenna, *Coord. Chem. Rev.*, 2016, **311**, 53–74.
17 G. A. Ardizzoia, S. Brenna, S. Durini, B. Therrien and M. Veronelli, *Eur. J. Inorg. Chem.*, 2014, 4310–4319.
18 G. A. Ardizzoia, S. Brenna, S. Durini and B. Therrien, *Polyhedron*, 2015, **90**, 214–220.
19 G. A. Ardizzoia, G. Colombo, B. Therrien and S. Brenna, *Eur. J. Inorg. Chem.*, 2019, 1825–1831.
20 S. Durini, G. A. Ardizzoia, B. Therrien and S. Brenna, *New J. Chem.*, 2017, **41**, 3006–3014.
21 G. A. Ardizzoia, S. Brenna, F. Civati, V. Colombo and A. Sironi, *CrystEngComm*, 2017, **19**, 6020–6027.
22 S. Durini, G. A. Ardizzoia, G. Colombo, B. Therrien and S. Brenna, *Polyhedron*, 2018, **139**, 189–195.
23 P. D. Harvey, M. Drouin and T. Zhang, *Inorg. Chem.*, 1997, **36**, 4998–5005.
24 B.-F. Ruan, R.-T. Hu, Y.-P. Tian, J.-Y. Wu and H.-L. Zhu, *J. Coord. Chem.*, 2010, **63**, 2999–3005.
25 T. Nishi and T. Tsubomura, *Chem. Lett.*, 2018, **47**, 269–271.
26 L.-H. He, Y.-S. Luo, B.-S. Di, J.-L. Chen, C.-L. Ho, H.-R. Wen, S.-J. Liu, J.-Y. Wang and W.-Y. Wong, *Inorg. Chem.*, 2017, **56**, 10311–10324.

27 W.-W. Fan, Z.-F. Li, J.-B. Li, Y.-P. Yang, Y. Yuan, H.-Q. Tang, L.-X. Gao, Q.-H. Jin, Z.-W. Zhang and C.-L. Zhang, *J. Mol. Struct.*, 2015, **1099**, 351–358.
28 L. Yang, D. R. Powell and R. P. Houser, *Dalton Trans.*, 2007, 955–964.
29 M. Panera, J. Díez, I. Merino, E. Rubio and M. P. Gamasa, *Eur. J. Inorg. Chem.*, 2011, 393–404.
30 K.-B. Shiu, S.-A. Liu and G.-H. Lee, *Inorg. Chem.*, 2010, **49**, 9902–9908.
31 J.-L. Chen, Y.-L. Xiao, Y. Xia, L. Qiu, L.-H. He, S.-J. Liu and H.-R. Wen, *Polyhedron*, 2016, **112**, 130–136.
32 D. Li, X. Sun, N. Shao, G. Zhang, S. Li, H. Zhou, J. Wu and Y. Tian, *Polyhedron*, 2015, **93**, 17–22.
33 J. Ruiz, M. P. Gonzalo, M. Vivanco, R. Quesada and M. E. G. Mosquera, *Dalton Trans.*, 2009, 9280–9290.
34 W. Shi, L. Zhang, M. Shafaei-Fallah and A. Rothenberger, *Z. Anorg. Allg. Chem.*, 2007, **633**, 2431–2434.
35 C. E. Anson, L. Ponikiewski and A. Rothenberger, *Inorg. Chim. Acta*, 2006, **359**, 2263–2267.
36 K. Jiang, D. Zhao, L.-B. Guo, C.-J. Zhang and R.-N. Yang, *Chin. J. Chem.*, 2004, **22**, 1297–1302.
37 R. Yang, Y. Sun, D. Zhao and L. Guo, *J. Coord. Chem.*, 2003, **56**, 1169–1177.
38 A. M. Manotti Lanfredi, F. Uguzzoli, A. Camus, N. Marsich and R. Capelletti, *Inorg. Chim. Acta*, 1993, **206**, 173–185.
39 A. Bondi, *J. Phys. Chem.*, 1964, **68**, 441–451.
40 N. V. Belkova, I. E. Golub, E. I. Gutsul, K. A. Lyssenko, A. S. Peregudov, V. D. Makhaev, O. A. Filippov, L. M. Epstein, A. Rossin, M. Peruzzini and E. S. Shubina, *Crystals*, 2017, **7**, 318–334.
41 A. W. Cook, T.-A. D. Nguyen, W. R. Buratto, G. Wu and T. W. Hayton, *Inorg. Chem.*, 2016, **55**, 12435–12440.
42 W. J. Geary, *Coord. Chem. Rev.*, 1971, **7**, 81–122.
43 S. Shi, M. Chul Jung, C. Coburn, A. Tadle, D. Sylvinson M. R., P. I. Djurovich, S. R. Forrest and M. E. Thompson, *J. Am. Chem. Soc.*, 2019, **141**, 3576–3588.
44 V. A. Krylova, P. I. Djurovich, J. W. Aronson, R. Haiges, M. T. Whited and M. E. Thompson, *Organometallics*, 2012, **31**, 7983–7993.
45 C.-H. Li, S. Chi Fai Kui, I. Hiu Tung Sham, S. Sin-Yin Chui and C.-M. Che, *Eur. J. Inorg. Chem.*, 2008, 2421–2428.
46 S. D. Cummings and R. Eisenberg, *Inorg. Chem.*, 1995, **34**, 2007–2014.
47 C. Makedonas, C.-A. Mitsopoulou, F. J. Lahoz and A. I. Balana, *Inorg. Chem.*, 2003, **42**, 8853–8865.
48 M. Al-Noaimi, M. I. El-Barghouthi, O. S. Abdel-Rahman, S. F. Haddad and A. M. Rawashdeh, *Polyhedron*, 2011, **30**, 1884–1890.
49 M. A. Omary and H. H. Patterson, *Inorg. Chem.*, 1998, **37**, 1060–1066.
50 G. So Ming Tong, S. Chi Fai Kui, H.-Y. Chao, N. Zhu and C.-M. Che, *Chem. – Eur. J.*, 2009, **15**, 10777–10789.
51 K. N. Jarzembska, R. Kamiński, B. Fournier, E. Trzop, J. D. Sokolow, R. Henning, Y. Chen and P. Coppens, *Inorg. Chem.*, 2014, **53**, 10594–10601.
52 J. Nitsch, F. Lacemon, A. Lorbach, A. Eichhorn, F. Cisnetti and A. Steffen, *Chem. Commun.*, 2016, **52**, 2932–2935.
53 M. El Sayed Moussa, S. Evariste, H.-L. Wong, L. Le Bras, C. Roiland, L. Le Polles, B. Le Guennic, K. Costuas, V. W.-W. Yam and C. Lescop, *Chem. Commun.*, 2016, **52**, 11370–11373.
54 A. Belyaev, T. Eskelinen, T. Minh Dau, Y. Y. Ershova, S. P. Tunik, A. S. Melnikov, P. Hirva and I. O. Koshevoy, *Chem. – Eur. J.*, 2018, **24**, 1404–1415.
55 H. V. Rasika Dias, H. V. K. Diyabalanage, M. G. Eldabaja, O. Elbjeirami, M. A. Rawashdeh-Omary and M. A. Omary, *J. Am. Chem. Soc.*, 2005, **127**, 7489–7501.
56 C.-M. Che and S.-W. Lai, *Coord. Chem. Rev.*, 2005, **249**, 1296–1306.
57 G. M. Sheldrick, *Acta Crystallogr., Sect. C: Struct. Chem.*, 2015, **71**, 3–8.
58 L. J. Farrugia, *J. Appl. Crystallogr.*, 1997, **30**, 565.
59 (*a*) G. te Velde, F. M. Bickelhaupt, E. J. Baerends, C. Fonseca Guerra, S. J. A. van Gisbergen, J. G. Snijders and T. Ziegler, *J. Comput. Chem.*, 2001, **22**, 931–967; (*b*) C. Fonseca Guerra, J. G. Snijders, G. te Velde and E. J. Baerends, *Theor. Chem. Acc.*, 1998, **99**, 391–403; (*c*) E. J. Baerends, T. Ziegler, J. Autschbach, D. Bashford, A. Bérces, F. M. Bickelhaupt, C. Bo, P. M. Boerrigter, L. Cavallo, D. P. Chong, L. Deng, R. M. Dickson, D. E. Ellis, M. van Faassen, L. Fan, T. H. Fischer, C. Fonseca Guerra, M. Franchini, A. Ghysels, A. Giammona, S. J. A. van Gisbergen, A. W. Götz, J. A. Groeneveld, O. V. Gritsenko, M. Grüning, S. Gusarov, F. E. Harris, P. van den Hoek, C. R. Jacob, H. Jacobsen, L. Jensen, J. W. Kaminski, G. van Kessel, F. Kootstra, A. Kovalenko, M. V. Krykunov, E. van Lenthe, D. A. McCormack, A. Michalak, M. Mitoraj, S. M. Morton, J. Neugebauer, V. P. Nicu, L. Noodleman, V. P. Osinga, S. Patchkovskii, M. Pavanello, P. H. T. Philipsen, D. Post, C. C. Pye, W. Ravenek, J. I. Rodríguez, P. Ros, P. R. T. Schipper, H. van Schoot, G. Schreckenbach, J. S. Seldenthuis, M. Seth, J. G. Snijders, M. Solà, M. Swart, D. Swerhone, G. te Velde, P. Vernooijs, L. Versluis, L. Visscher, O. Visser, F. Wang, T. A. Wesolowski, E. M. van Wezenbeek, G. Wiesenekker, S. K. Wolff, T. K. Woo and A. L. Yakovlev, *ADF2017, SCM, Theoretical Chemistry*, Vrije Universiteit, Amsterdam, The Netherlands, http://www.scm.com.
60 S. Grimme, J. Antony, S. Ehrlich and S. Krieg, *J. Chem. Phys.*, 2010, **132**, 154104.
61 D. P. Chong, *Mol. Phys.*, 2005, **103**, 749–761.